

EUMETSAT Satellite Application Facility on
Support to Operational Hydrology and Water Management
<http://hsaf.meteoam.it/>



Product validation report (PVR)

H26

Soil Wetness Index in the roots region
by ASCAT soil moisture assimilation

Revision History

Revision	Date	Author(s)	Description
0.1	2024/04/24	David Fairbairn and Patricia de Rosnay	First version.

Table of Contents

1. Executive summary	7
2. Introduction	7
2.1. Purpose of the document	7
2.2. Targeted audience	7
3. Introduction to the root-zone soil wetness index product (H26)	7
3.1. Principal of the product	7
3.2. Main characteristics	8
3.3. Validation approach	9
4. Validation against in situ data	9
4.1. Introduction	9
4.2. In situ data	10
4.3. In situ data preparation and metrics	11
4.4. Validation results	12
5. Case study analysis	19
5.1. Introduction	19
5.2. Case study analysis in Belgium at RMIB	19
5.3. Case study analysis in Bulgaria (NIMH Sofia)	20
5.3.1. Introduction	20
5.3.2. Sensor locations	22
5.3.3. Data processing	22
5.3.4. Statistical results	23
6. Conclusion	24
7. References	24
Appendices	28
A. Introduction to H SAF	28
B. Purpose of the H SAF	28
C. Products / Deliveries of the H SAF	29
D. System Overview	30

List of Tables

4.1.	Pearson correlation coefficient performance requirements for H26 [R]	10
4.2.	Mean scores for the H26 surface (top) and root-zone (bottom) SWI layers against in situ measurements from the SCAN, USCRN, SNOTEL, SMOSMANIA, REMED-HUS and TERENO networks.	16
4.3.	Mean seasonal scores for the H26 surface SWI layer against in situ measurements from all the networks. The summer, autumn, spring and winter seasons are represented by the periods June to August, September to November, March to May and December to February respectively. Also shown are the number of stations for each network and season (Summer/Autumn/Winter/Spring)	16
4.4.	Same as Table 4.3 but for the root-zone SWI	18
5.1.	Average statistics for the period 2022/03/23-2023/05/31	23
5.2.	Results by automatic station equipped with CS650, CS655 or ENVIROSCAN Sensors.	23
5.3.	Seasonal statistics for the period 2022/03/23-2023/05/31.	23

List of Figures

3.1.	Illustration of the H26 root zone soil moisture production chain based on ASCAT-B/C satellite derived surface soil moisture data assimilation in the SSA configuration. The highlighted box encompasses the coupled land-atmosphere 12-hour first guess.	8
4.1.	Locations of the stations of the US (top-left), German (top-right), French (bottom-left), and Spanish (bottom-right) networks used in the validation. Also shown is the correlation coefficient averaged over the period for each station.	14
4.2.	Illustration of soil moisture products time series for a station belonging to the TERENO network for a) Surface SM and b) Root-zone SM. The in situ data are in blue and H26 is in red.	15
4.3.	Box plots of correlation and anomaly correlation coefficients between in situ observations and H26 for March 2021 to May 2023. The surface SM scores are on the left and the root-zone SM scores are on the right.	17
4.4.	Pearson R anomalies for each network over the validation period. The left plot shows surface SWI scores and the right plot shows root-zone SWI scores.	18
5.1.	Map of Belgium with the watershed of the Demer at Molenstede.	20
5.2.	Time series of H26 vs SCHEME for (a) upper and (b) lower layers.	21
5.3.	Map of Bulgaria with the locations of the automatic sensors.	22
A.1.	Conceptual scheme of the EUMETSAT Application Ground Segment.	28
A.2.	Current composition of the EUMETSAT SAF Network.	29

List of Acronyms

ASAR	Advanced Synthetic Aperture Radar (on Envisat)
ASAR GM	ASAR Global Monitoring
ASCAT	Advanced Scatterometer
ATBD	Algorithm Theoretical Baseline Document
BUFR	Binary Universal Form for the Representation of meteorological data
DORIS	Doppler Orbitography and Radiopositioning Integrated by Satellite (on Envisat)
ECMWF	European Centre for Medium-range Weather Forecasts
ERS	European Remote-sensing Satellite (1 and 2)
ESA	European Space Agency
EUMETCast	EUMETSAT's Broadcast System for Environment Data
EUMETSAT	European Organisation for the Exploitation of Meteorological Satellites
FTP	File Transfer Protocol
HTESSEL	Hydrology Tiled ECMWF Scheme of Surface Exchanges over Land
H SAF	SAF on Support to Operational Hydrology and Water Management
LDAS	Land Data Assimilation System
Météo France	National Meteorological Service of France
Metop	Meteorological Operational Platform
NRT	Near Real-Time
NWP	Numerical Weather Prediction
PRD	Product Requirements Document
PUM	Product User Manual
PVR	Product Validation Report
SAF	Satellite Application Facility
SEKF	Simplified Extended Kalman Filter
SSM	Surface soil moisture
SWI	Soil Wetness Index
TU Wien	Technische Universität Wien (Vienna University of Technology)

WARP Soil Water Retrieval Package

WARP H WARP Hydrology

WARP NRT WARP Near Real-Time

ZAMG Zentralanstalt für Meteorologie und Geodynamik (National Meteorological Service of Austria)

1. Executive summary

This document describes the validation of the near-real-time (NRT) H SAF scatterometer root zone soil moisture 10 km resolution product (RZSM-ASCAT-NRT-10km/H26) for the operational review 13. It is validated over the period March 23rd 2021 to May 31st 2023. An introduction (section 2) is followed by general overview of the H SAF root zone near-real-time product (section 3). The product validation of the entire root-zone (0-1 m depth) against sparse in situ data is presented in section 4. Case studies for a hydrological application in Belgium and for a SM validation over Bulgaria are presented in Section 5. Finally, the conclusion is given in section 6.

Further information on the implementation of the processing chain and individual processing steps are available in the H26 Algorithm Theoretical Basis Documents [1], and information on the product format can be found in the H26 Product User Manual [2]. A pre-operational validation of H26 was also performed for the operational readiness review [3]. Information about the H SAF consortium can be found in the Appendix.

2. Introduction

2.1. Purpose of the document

The Product Validation Report is intended to provide a description of the main product characteristics and validation results for RZSM-ASCAT-NRT-10km (H26). The validation approach adopted for H26 will include the temporal correlation of the root zone soil moisture against in situ measurements from the International Soil Moisture Network [4] in Section 4. Only the top 3 layers of the root-zone are validated using in situ observations (0-100 cm depth), which correspond with the analyzed soil moisture layers in the SEKF data assimilation algorithm. The lack of in situ data below 100 cm depth means it is not feasible to validate the deepest layer between 100 and 289 cm depth. The validation period is from March 23rd 2022 (the date when H26 became operational) to May 31st 2023. During this period the H SAF ASCAT-B/C SSM products (H103/H105) were available for assimilation. It is worth noting that the ASCAT-A (H102) product was retired before H26 became operational.

2.2. Targeted audience

This document mainly targets:

- Hydrology and water management experts
- Operational hydrology and Numerical Weather Prediction communities
- Users of remotely sensed soil moisture for a range of applications (e.g. climate modelling validation, trend analysis)

3. Introduction to the root-zone soil wetness index product (H26)

3.1. Principal of the product

The H26 production chain uses a sequential Land Data Assimilation System (LDAS) based on a Simplified Extended Kalman Filter (SEKF) method, as in [5]. The SEKF constitutes

the central component of the H26 production chain. The H-TESSEL Land Surface Model is used to propagate in time and space the soil moisture information through the root zone, accounting for physiographic information (soil texture, orography), meteorological conditions and land surface processes such as soil evaporation and vegetation transpiration [6–8]. H26 is a root zone soil moisture product derived from Metop ASCAT-B/C surface soil moisture (SSM) observations. The retrieval approach relies on a sequential Land Data Assimilation System (LDAS) with 12-hour assimilation windows. The LDAS for H26 is implemented using the "stand-alone surface analysis" (SSA) configuration of [9]. The atmospheric analysis is forced from the archived operational 9 km ECMWF analysis, but the LDAS and coupled first guess are performed independently. Figure 3.1 illustrates the H26 production suite.

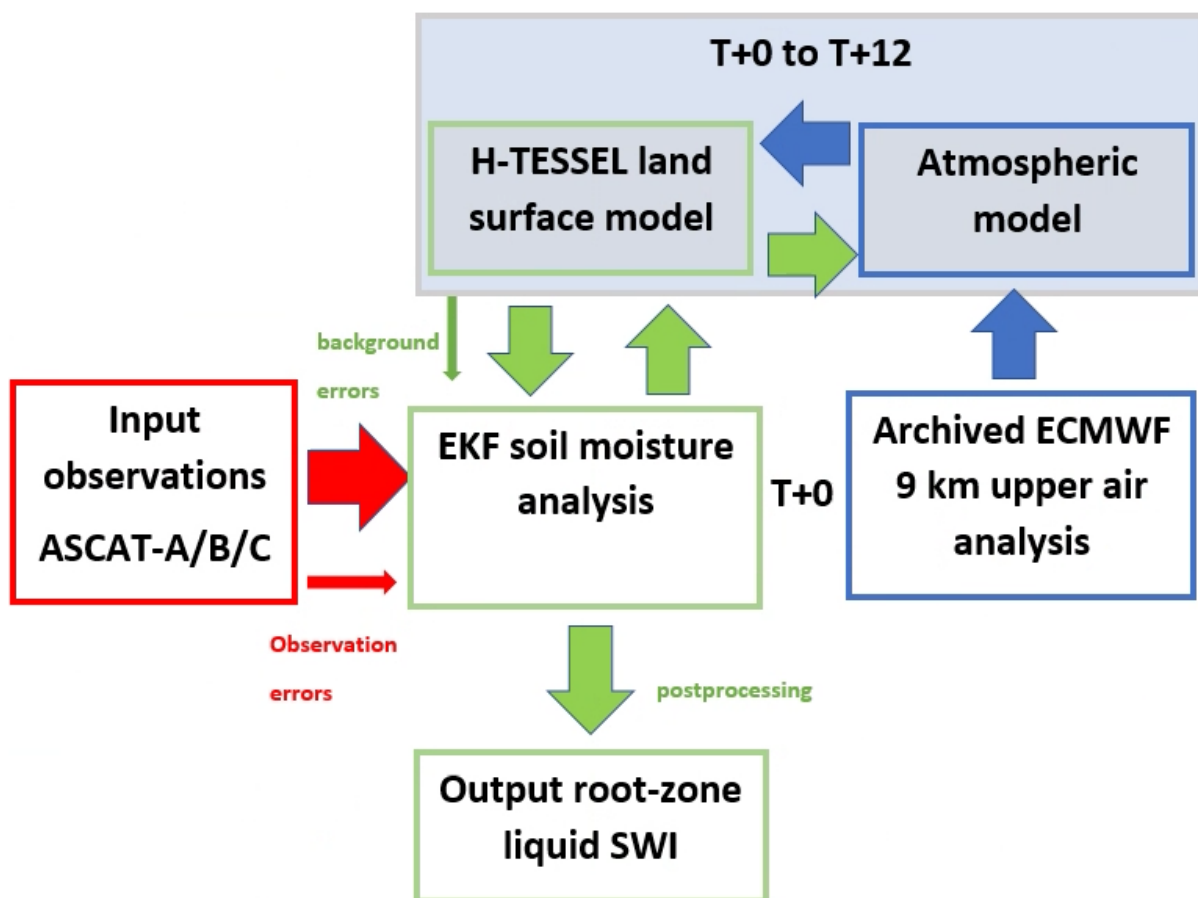


Figure 3.1: Illustration of the H26 root zone soil moisture production chain based on ASCAT-B/C satellite derived surface soil moisture data assimilation in the SSA configuration. The highlighted box encompasses the coupled land-atmosphere 12-hour first guess.

3.2. Main characteristics

H26 is a daily NRT product valid at 00UTC and with a timeliness of 12 hours i.e. the 00 UTC output should arrive on the H SAF ftp no later than 12 UTC. H26 is produced at a horizontal

resolution of about 10km on four vertical layers in the soil: surface to 7 cm, 7 cm to 28 cm, 28 cm to 100 cm, and 100 cm to 289 cm. H26 relies on a data assimilation approach that propagates the information in time and space (on the vertical dimension in the root zone). Therefore, it allows a global update of the root zone soil moisture states using SSM derived from the aforementioned ASCAT products. The H26 root-zone soil moisture product is expressed as a liquid soil wetness index, with units between 0 (zero soil moisture) and 1 (saturation), representing the lower and upper soil moisture limits. After data assimilation, a post-processing step is required to convert the volumetric soil moisture analysis into the soil wetness index. It is computed using the soil texture (as defined by the FAO/United Nations Educational, Scientific and Cultural Organization (UNESCO) Digital Soil Map of the world [10]), the saturated soil moisture, and the fraction of liquid water content (the fraction of water that is not frozen) on each grid point and each soil layer. Having the units of H26 as a liquid soil wetness index is consistent with all the other ASCAT soil moisture products that are available for the surface (e.g. H141 and H102). Furthermore, it is relevant to various applications and can be combined with different hydrological models (e.g. [11]).

3.3. Validation approach

Several authors have demonstrated that in situ soil moisture measurements could be used to validate model and remotely-sensed SM at different scales (e.g. [12–14]). The high spatial variability of in situ SM used for validation as well as SM data set specific characteristics suggests that the Pearson correlation coefficient (R) should be the main score to be evaluated. Supportive scores are the Root Mean Square Difference (RMSD), Mean Error (or bias, ME), and the Standard Deviation (SD). Table 4.1 demonstrates the accuracy requirements for the RZSM. Cases with significant levels of correlations ($p\text{-value} < 0.05$) are considered only as discussed in section 4.3.

Two validations are performed: (i) the validation against in situ data from the ISMN and (ii) Case study analysis. Both components (long statistical and case study analysis) are considered complementary in assessing the accuracy of the implemented algorithms. The in situ validation helps in identifying the possible existence of a pathological behaviour, while selected case studies are useful in identifying the roots of such behaviour, when present.

4. Validation against in situ data

4.1. Introduction

Data from 6 networks in the ISMN are considered for the validation. Three networks are located in the US: NRCS-SCAN (Natural Resources Conservation Service - Soil Climate Analysis Network), USCRN (U.S. Climate Reference Network) and NRCS-SNOTEL (short for Snow Telemetry) [15, 16]. The SMOSMANIA (Soil Moisture Observing System Meteorological Automatic Network Integrated Application) network [17, 18] is located over southwest France. The TERENO (Network of Terrestrial Environmental Observatories in Germany) network [19] is located in northwest Germany. Additionally, the REMEDHUS network in Spain [20] is employed to validate the surface layer. Despite this geographical extent limitation, these networks sample a large diversity of soil and vegetation types. They cover most of the soil texture and vegetation types (forest, crops, natural fallow, bare soil) in plains, mountainous, and coastal areas. More information about the networks is given in Section 4.2.

Table 4.1: Pearson correlation coefficient performance requirements for H26 [R]

Unit	Threshold	Target	Optimal
Dimensionless	0.5	0.65	0.8

4.2. In situ data

This study makes use of in situ soil moisture measurements obtained through the International Soil Moisture Network (ISMN ¹, [4, 21]), a data hosting centre where globally-available ground-based soil moisture measurements are collected, harmonized and made available to users. The performance of H26 is estimated by comparing it with in situ observations from 6 in situ networks in the US and Europe. A description of each network is given below together with the total number of stations used after quality control screening.

The NRCS-SCAN network [15] is a comprehensive, USA-wide soil moisture and climate information system designed to provide data to support natural resource assessments and conservation activities with a focus on agricultural areas in the USA. The observing network is used to monitor soil temperature and soil moisture at several depths, soil water level, air temperature, relative humidity, solar radiation, wind, precipitation and barometric pressure amongst other variables. NRCS-SCAN data have been used for various studies ranging from global climate modelling to agricultural studies. The vegetation cover at these sites consists of either natural fallow or short grass. Data are collected by a dielectric constant measuring device and typically measurements are made at 5, 10, 20, 50 and 100 cm. After the quality control checks, a sample of 118 out of 207 stations was used in the validation.

The U.S. Climate Reference Network National from the Oceanic and Atmospheric Administration's National Climatic Data Center (USCRN NOAA's NCDC) consists of stations developed, deployed, managed, and maintained by the National Oceanic and Atmospheric Administration (NOAA) in the contiguous United States for the express purpose of detecting the national signal of climate change [16]. The USCRN network is spread across many parts of the USA, from North to South and West to East (network map available on the ISMN website). USCRN sites sample a variety of natural environments in addition to agricultural settings that predominate in some networks. The main objective of USCRN is to provide climate-science-quality measurements of air temperature and surface conditions. The stations in the network were designed to be extensible to other missions and in 2011, the USCRN team completed at each station in the contiguous United States the installation of triplicate-configuration soil moisture and soil temperature probes at 5, 10, 20, 50, and 100 cm. After the quality control checks, a sample of 103 out of 112 stations was used in the validation.

The Natural Resources Conservation Service (NRCS) installs, operates and maintains an extensive, automated system called SNOTEL (short for Snow Telemetry, [15, 16]). The SNOTEL is designed to collect snowpack and related climatic data in the Western U.S. and Alaska. Most of the stations also measure soil moisture and are located in high altitudes. Data are collected by a dielectric constant measuring device and typically measurements are made at 5, 20 and 50 cm. After the quality control checks, a sample of 241 out of 346 stations was used in the validation.

The SMOSMANIA project is a long-term data acquisition effort of soil moisture observations in Southwestern France [17, 18]. Soil moisture profile measurements at 12 automated

¹<https://ismn.geo.tuwien.ac.at/en/>

weather stations of Meteo-France from the RADOME network (Réseau d'Acquisition de Données d'Observations Météorologiques Etendu), have been obtained since January 2007 at four different depths (5, 10, 20 and 30 cm) with 12 minutes time steps. Stations span from the Mediterranean Sea to the Atlantic Ocean. The soil moisture measurements (in units of m^3m^{-3}) are derived from capacitance probes: ThetaProbe ML2X of Delta-T Devices. Data was kindly provided by J.-C. Calvet from Meteo-France in the framework of the HSAF project. After the quality control checks, a sample of 17 out of 21 stations was used in the validation.

The REMEDHUS is located in the central sector of the Duero basin in Spain. Each station has been equipped with capacitance probes (Stevens Hydraprobe) installed horizontally at a depth of 5 cm. Analysis of soil samples were carried out to verify the capacitances probes and to assess soil properties at each station [22]. After the quality control checks, a sample of 15 out of 18 stations was used in the validation.

Finally, the TERENO observations are located in the Eifel/Lower Rhine Valley in Germany [19]. Each station is equipped with capacitance probes (Stevens Hydraprobe) installed at depths of 5, 10 and 50 cm. After the quality control checks, 1 out of 4 stations was used in the validation.

4.3. In situ data preparation and metrics

Observations of soil moisture closest to the analysis time (± 30 minutes) are compared with the H26 soil moisture using the nearest neighbour approach. The rescaled in situ observations at the highest depth are used for the validation of the H26 surface layer (0-7 cm). The root-zone in situ soil moisture observations are approximated using a vertical average of the in situ measurements in the first metre of soil, with weights that are proportional to the spacing of the sensor depths (as in [23]). The REMEDHUS network is only used to validate the surface layer of H26, since deeper observations are not available from this network. For the SMOSMANIA (TERENO) networks, the deepest observations at 30 (50) cm are assumed to represent the depth 30-100 cm (50-100 cm). The rescaled root-zone in situ observations are then used to validate the average H26 root-zone soil wetness index (0-100 cm). H26 is an index between 0 and 1 while in situ measurements of soil moisture are in m^3m^{-3} . To enable a fair comparison, it is then necessary to rescale the data. The 90% confidence interval was chosen to define the upper and lower values to exclude any abnormal outliers due to instrument noise using the following equations (as in [13, 24]):

$$\begin{aligned}\text{Int}^+ &= \mu_{\text{in-situ}} + 1.64\sigma_{\text{in-situ}} \\ \text{Int}^- &= \mu_{\text{in-situ}} - 1.64\sigma_{\text{in-situ}},\end{aligned}\tag{1}$$

where Int^+ and Int^- are the upper and lower limits of the 90% confidence interval (i.e. 5th and 95th percentiles) calculated over the March 23rd 2022 to May 31st 2023 period. Then the SWI is obtained using:

$$\text{SWI} = \frac{\text{SM} - \text{Int}^-}{\text{Int}^+ - \text{Int}^-},\tag{2}$$

where SM stands for Soil Moisture (in volumetric units). It is assumed that the H26 data set does not have such a problem with outliers and is rescaled using the maximum and the minimum values of each individual times series considering the whole validation time period.

The comparison between the observation data and the H26 product is performed according to the following statistical scores:

- Mean difference (or Bias)
- Pearson Correlation coefficient (R)
- Anomaly correlation coefficient (Ranom)
- Root Mean Square Difference (RMSD). In situ data contain errors (instrumental and representativeness) so they are not considered as ‘true’ soil moisture. This is underlined here by using the RMS Difference terminology instead of RMS Error.
- p-value, a measure of the correlation significance should be calculated as well. It indicates the significance of the test, the 95% confidence interval should be used; configurations where the p-value is below 0.05 (i.e. the correlation is not a coincidence) have to be retained. This process has probably removed some good stations too (e.g., in areas where the model might not realistically represent soil moisture). However it also ensures that stations with non-significant R values can be considered suspect and are excluded from the computation of the network average metrics. It is commonly used for soil moisture validation activities against in situ as well as against model data sets [25,26].

The RMSD represents the relative error of the soil moisture dynamical range. As H26 is an index, it has no units. It is possible to obtain an estimate of the error of the liquid root zone soil moisture retrieval in m^3m^{-3} by multiplication between the RMSD and the observed dynamical range ($\text{obs}_{\text{max}} - \text{obs}_{\text{min}}$). Usually, soil moisture time series show a strong seasonal pattern that could artificially increase the perceived agreement between satellite and in situ observations in terms of CC. Therefore, to avoid seasonal effects, time series of anomalies from a moving monthly average are also calculated [13]. The difference to the mean is calculated for a sliding window of five weeks (if there are at least five measurements in this period), and the difference is scaled to the standard deviation. For each SM estimate at day (i), a period F is defined, with $F=[i-17, i+17]$ (corresponding to a 5-week window). If at least five measurements are available in this period of time, the average SM value and the standard deviation are calculated. The Anomaly (dimensionless) is then given by:

$$\text{Ano}(i) = \frac{\text{SM}(i) - \text{SM}(F)}{\text{stdev}(\text{SM}(F))}. \quad (3)$$

The anomaly transformation is used only to compute the Ranom scores. All the other metrics (ME, R, RMSD) are computed using the H26 time series without the anomaly transformation.

More often than not, soil moisture is measured along with soil temperature. In line with the validation of the first operational NRT product (SM-DAS-2/H14), the quality of H26 is assessed for all weather conditions, except when the soil temperature is below $+4^\circ\text{C}$. In addition, the 95% statistical significance intervals of the Ranom are calculated using a Fisher-Z transform (as in [27]). Note that the effective sampling size in the calculation of the confidence intervals is reduced by accounting for the temporal auto-correlation ([27] gives details).

4.4. Validation results

Firstly, maps are presented in Figure 4.1 showing the locations of the stations in each network used in the validation. On the maps, the average R over the entire validation period for H26 is shown for the surface SWI layer for each station. Recall that the performance requirements

for the correlation coefficients are listed in Table 4.1. While there is evidently some spatial variability in the performance across all 6 networks, most of the stations demonstrate R values above the target requirement ($CC > 0.65$). Similarly spatially distributed R scores were found for the root-zone (not shown).

Figure 4.2 illustrates a time series for the surface SM and the root-zone SM for the mid-latitude station of the TERENO network in Germany. At this latitude, SM exhibits significant seasonal-scale variability, with normally drier conditions in summer and wetter conditions during the winter. The surface SM variability is largely driven by the short-term atmospheric forcing e.g. precipitation events. The root-zone SM has a longer memory than the surface SM and the annual cycle should be more distinct. It is evident in Figure 4.2 that the soil moisture annual cycle as well as its short term variability is well represented in both layers i.e. most peaks and troughs. H26 is represented for the validation period from March 23rd 2022 until May 31st 2023.

Spatially averaged results of the H26 surface soil wetness validation against the in situ measurements for each network are reported at the top of Table 4.2. On average, the R scores are above the target performance of 0.65 for both layers. The Ranom scores are generally lower than the R scores, which is expected because the autocorrelation in the annual SM cycle is reflected in the Pearson R, but not in the anomalies. Nevertheless, the Ranom scores generally reach the threshold requirement of 0.50. The estimated surface SWI volumetric RMSDs are reasonable ($\approx 0.07 \text{ m}^3 \text{m}^{-3}$) and the biases are much smaller than the RMSDs. The root-zone SWI scores are given at the bottom of Table 4.2. Overall, the root-zone SWI performs slightly better than the surface SWI in terms of the R/Ranom and has a substantially smaller average RMSD. This is expected because the root-zone SWI is less sensitive to random errors in the atmospheric forcing than the surface SWI. Note that there are generally fewer stations used to validate the root-zone SWI than the surface SWI, since measurements across all the root-zone depths are needed to construct the root-zone layer and measurements are discarded if data is missing or if the temperature is below 4°C .

Table 4.3 reports statistical scores for the H26 surface SWI at a seasonal scale. R values are, on average, above the threshold (0.50) and targeted (0.65) values for all seasons. The spring period (March to May) demonstrated the highest average R (0.72) and the summer period (June to August) showed the lowest average R (0.67). Note that there is less data available in winter due to frozen conditions at some of the sites. Similarly, the root-zone SWI seasonal scores are given in Table 4.4. In this case, the highest average R (0.75) was in summer and the lowest average R (0.67) in winter.

Figure 4.3 displays box plots of the distribution of the R values across all the stations for the US and SMOSMANIA networks. Note that the REMEDHUS network is not shown because it is only valid for the surface, whilst the TERENO network only has one station available over the period. Five metrics are included, namely the median, upper quartile, lower quartile, minimum and maximum values (excluding outliers more/less than $3/2$ times the lower quartile). The left (right) hand side of Figure 4.3 shows box plots of the R for each network for the surface (root-zone) SM. For the US stations (labelled a-f), the interquartile range for the R spans between about 0.40 and 0.90 and the majority of stations are above the target accuracy requirement of 0.65. For the root-zone SM, more than 25% of stations exceed the optimum R value (0.8) for all of the networks. As expected, the anomaly correlations are generally lower than the correlations as the autocorrelations from the annual cycle are removed. Nevertheless, the median anomaly correlations consistently exceed the threshold requirement (0.50). The root-zone SWI correlations are generally slightly higher than the surface SWI correlations.

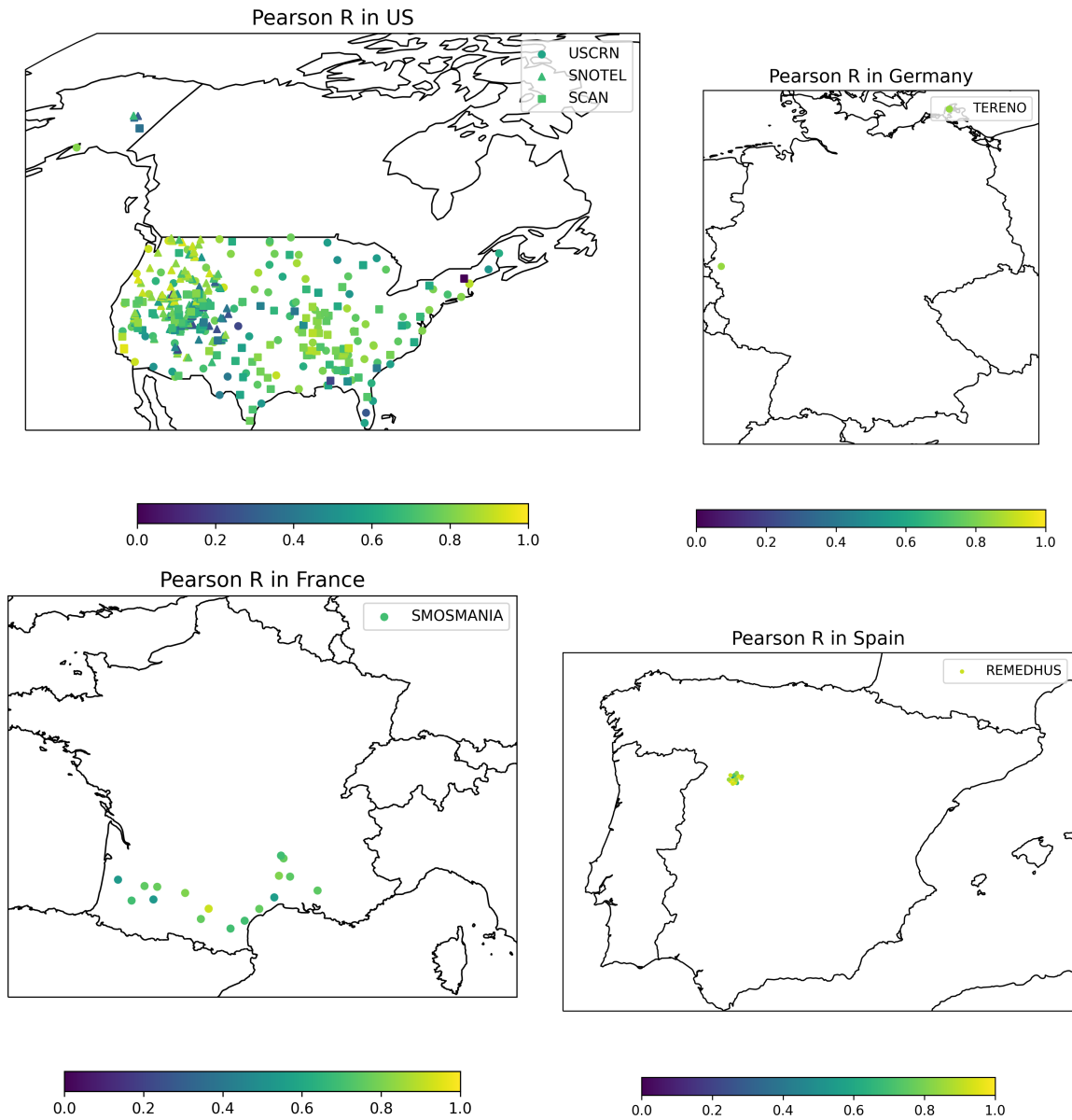


Figure 4.1: Locations of the stations of the US (top-left), German (top-right), French (bottom-left), and Spanish (bottom-right) networks used in the validation. Also shown is the correlation coefficient averaged over the period for each station.

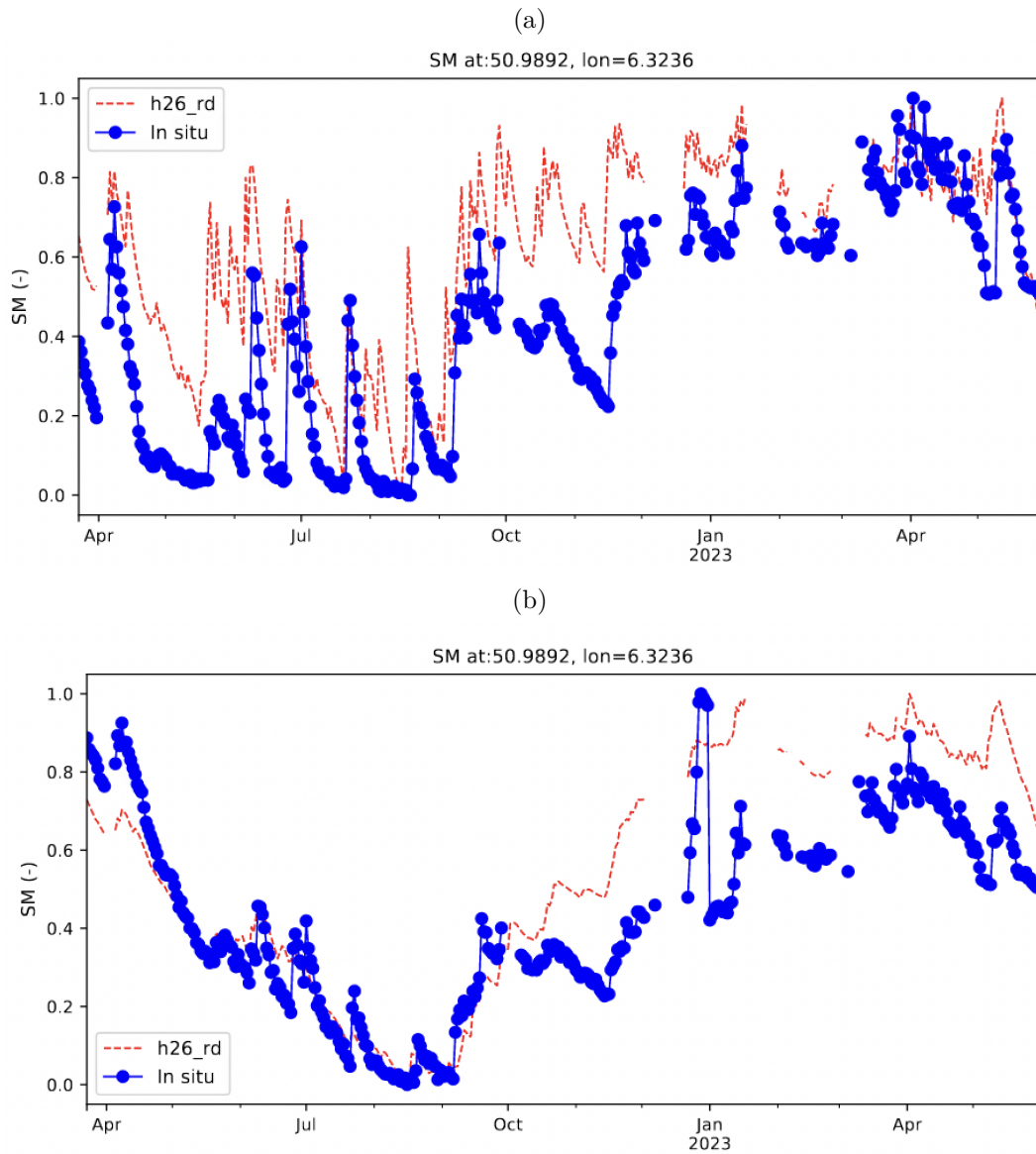


Figure 4.2: Illustration of soil moisture products time series for a station belonging to the TERENO network for a) Surface SM and b) Root-zone SM. The in situ data are in blue and H26 is in red.

Table 4.2: Mean scores for the H26 surface (top) and root-zone (bottom) SWI layers against in situ measurements from the SCAN, USCRN, SNOTEL, SMOSMANIA, REMEDHUS and TERENO networks.

Surface SM scores				
Network (N stations)	R	Ranom	RMSD (m^3m^{-3})	Bias (m^3m^{-3})
SCAN (118)	0.68	0.49	0.07	0.01
USCRN (103)	0.73	0.55	0.06	0.02
SNOTEL (241)	0.68	0.49	0.07	0.00
SMOSMANIA (17)	0.72	0.56	0.07	0.05
REMEDHUS (15)	0.85	0.32	0.04	0.01
TERENO (1)	0.84	0.64	0.08	0.06
Average	0.70	0.50	0.07	0.01

Root-zone SM scores				
Network (N stations)	R	Ranom	RMSD (m^3m^{-3})	Bias (m^3m^{-3})
SCAN (100)	0.71	0.51	0.04	0.00
USCRN (93)	0.73	0.52	0.04	0.00
SNOTEL (216)	0.77	0.53	0.04	0.00
SMOSMANIA (12)	0.73	0.62	0.04	0.02
TERENO (1)	0.87	0.69	0.02	0.01
Average	0.75	0.53	0.04	0.00

Table 4.3: Mean seasonal scores for the H26 surface SWI layer against in situ measurements from all the networks. The summer, autumn, spring and winter seasons are represented by the periods June to August, September to November, March to May and December to February respectively. Also shown are the number of stations for each network and season (Summer/Autumn/Winter/Spring)

Network (N stations)	Score	Summer	Autumn	Winter	Spring
SCAN (75/96/54/99)	Bias (m^3m^{-3})	0.01	0.01	0.02	0.01
	RMSD (m^3m^{-3})	0.07	0.06	0.05	0.07
	R (anomalies)	0.59 (0.48)	0.71 (0.61)	0.68 (0.48)	0.69 (0.69)
USCRN (43/54/55/31)	Bias (m^3m^{-3})	0.01	0.02	0.02	0.03
	RMSD (m^3m^{-3})	0.07	0.06	0.05	0.06
	R (anomalies)	0.65 (0.49)	0.69 (0.63)	0.69 (0.70)	0.71 (0.60)
SNOTEL (191/206/1/110)	Bias (m^3m^{-3})	0.01	-0.01	-0.01	-0.03
	RMSD (m^3m^{-3})	0.07	0.06	0.01	0.08
	R (anomalies)	0.71 (0.48)	0.68 (0.66)	0.99 (0.99)	0.76 (0.65)
SMOSMANIA (13/13/15/16)	Bias (m^3m^{-3})	0.04	0.07	0.05	0.05
	RMSD (m^3m^{-3})	0.06	0.08	0.05	0.06
	R (anomalies)	0.66 (0.52)	0.68 (0.53)	0.69 (0.74)	0.73 (0.69)
REMEDHUS (4/10/15/12)	Bias (m^3m^{-3})	-0.03	0.01	0.02	0.02
	RMSD (m^3m^{-3})	0.05	0.04	0.03	0.06
	R (anomalies)	0.43 (0.08)	0.88 (0.46)	0.73 (0.73)	0.79 (0.48)
TERENO (1/1/1/1)	Bias (m^3m^{-3})	0.06	0.09	0.05	0.05
	RMSD (m^3m^{-3})	0.08	0.10	0.05	0.07
	R (anomalies)	0.64 (0.61)	0.77 (0.70)	0.65 (0.56)	0.88 (0.67)

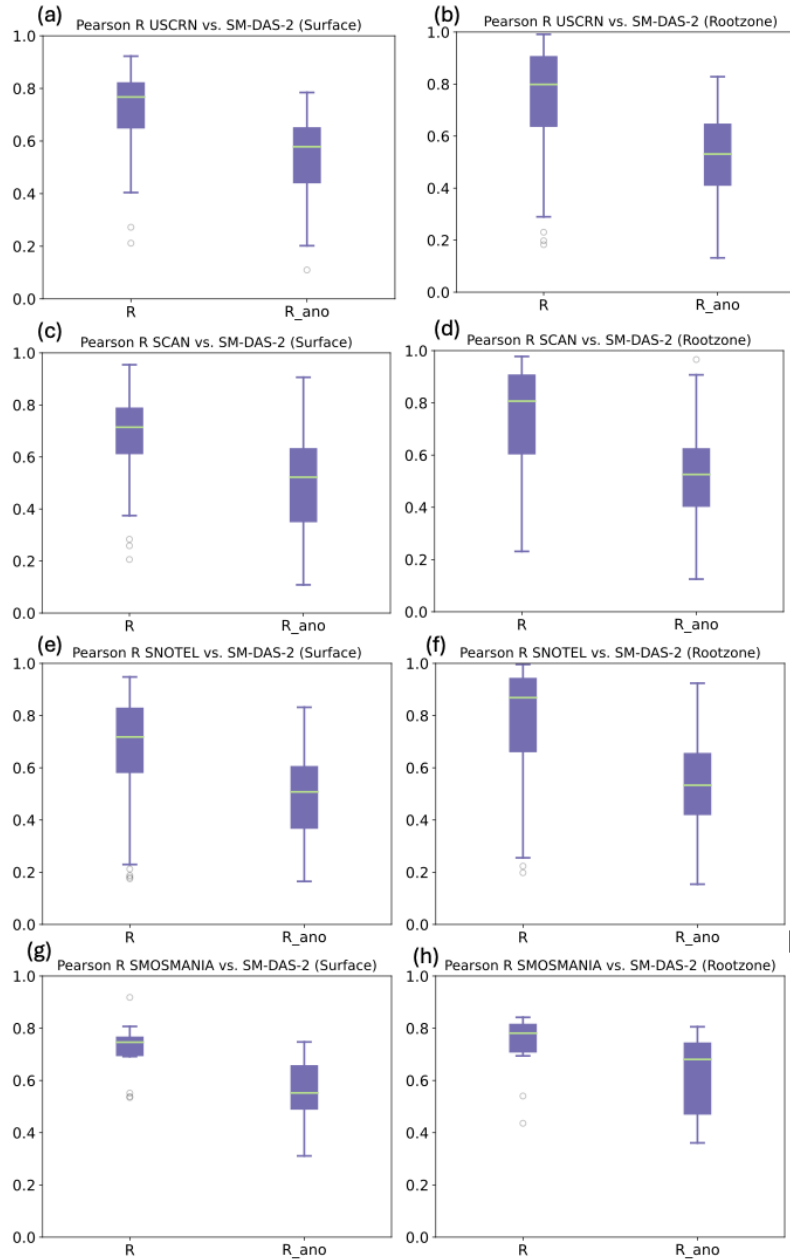


Figure 4.3: Box plots of correlation and anomaly correlation coefficients between in situ observations and H26 for March 2021 to May 2023. The surface SM scores are on the left and the root-zone SM scores are on the right.

Table 4.4: Same as Table 4.3 but for the root-zone SWI

Network (N stations)	Score	Summer	Autumn	Winter	Spring
SCAN (52/73/41/82)	Bias (m^3m^{-3})	-0.01	-0.01	0.00	0.01
	RMSD (m^3m^{-3})	0.04	0.03	0.04	0.04
	R (anomalies)	0.62 (0.50)	0.65 (0.62)	0.68 (0.72)	0.70 (0.62)
USCRN (68/74/31/82)	Bias (m^3m^{-3})	0.00	-0.01	0.01	0.01
	RMSD (m^3m^{-3})	0.04	0.04	0.05	0.05
	R (anomalies)	0.72 (0.53)	0.72 (0.58)	0.66 (0.64)	0.67 (0.60)
SNOTEL (202/158/0/73)	Bias (m^3m^{-3})	0.01	0.00	N.A.	-0.02
	RMSD (m^3m^{-3})	0.05	0.03	N.A.	0.05
	R (anomalies)	0.80 (0.54)	0.65 (0.64)	N.A.	0.84 (0.75)
SMOSMANIA (7/7/6/12)	Bias (m^3m^{-3})	0.03	-0.01	0.01	0.04
	RMSD (m^3m^{-3})	0.04	0.04	0.04	0.05
	R (anomalies)	0.45 (0.56)	0.84 (0.54)	0.73 (0.77)	0.78 (0.73)
TERENO (1/1/0/1)	Bias (m^3m^{-3})	0.00	0.01	N.A.	0.01
	RMSD (m^3m^{-3})	0.01	0.02	N.A.	0.02
	R (anomalies)	0.93 (0.59)	0.73 (0.85)	N.A.	0.70 (0.76)

Figure 4.4 shows the Ranom and 95% confidence intervals for (a) the surface layer and (b) the root-zone layer for each network. The H26 Ranom scores are mainly above the threshold (0.50) for both the surface and root-zone layers, with the exception of REMEDHUS, which performs rather poorly over the period. The large confidence intervals for SNOTEL are related to the lack of data available due to the frozen conditions over much of the period.

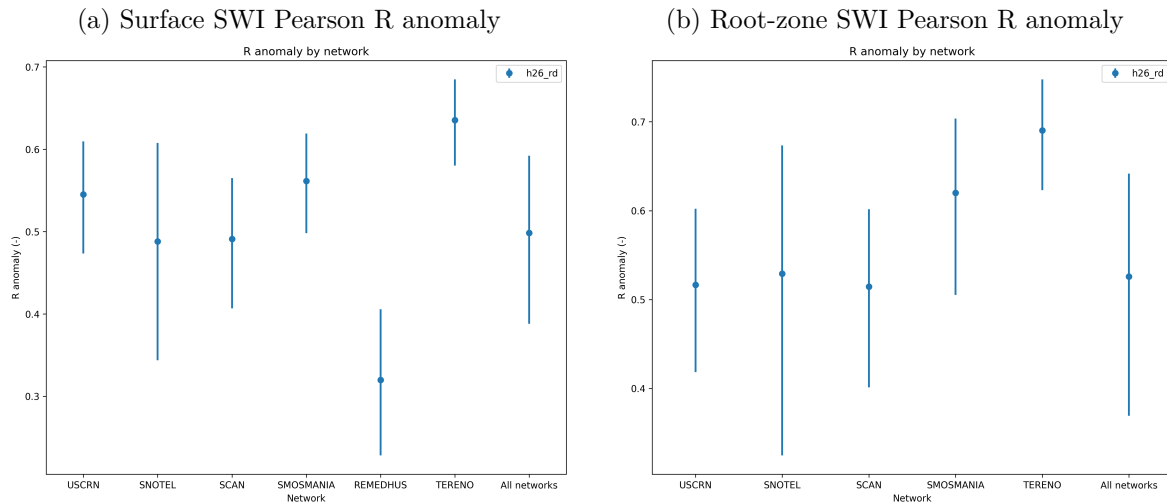


Figure 4.4: Pearson R anomalies for each network over the validation period. The left plot shows surface SWI scores and the right plot shows root-zone SWI scores.

5. Case study analysis

5.1. Introduction

The first case study is the comparison of H26 with the SCHEME hydrological model in Belgium, followed by an in situ soil moisture validation in Bulgaria.

5.2. Case study analysis in Belgium at RMIB

The Royal Meteorological Institute Belgium (RMIB) validation activity concerning the H26 product consists in its comparison with the soil moisture content of the two soil reservoirs in the SCHEME hydrological model. This is therefore a comparison from model to model even if both are using different information and the validation is indirectly achieved with the comparison of the streamflow simulated by the SCHEME hydrological model with the streamflow measured at the corresponding gauge station during the reference period. The SCHEME hydrological model (for SCHEldt and MEuse) is a semi-distributed version of the conceptual model developed by [28,29]. Evapotranspiration is estimated by depleting the content of conceptual reservoirs for water intercepted by vegetation and for two soil layers, in comparison with a potential value given by a Penmann formulation. As this model is aimed at simulating the hydrograph, the saturation threshold of the upper layer of the soil is optimized for the surface runoff during rainy periods in a calibration dataset whereas the saturation threshold of the zone of aeration is obtained by comparing the cumulated evapotranspiration and the deficit of flow over the reference period. The latter parameter is a function of the cover (seven vegetated covers are defined) and of the month. In the SCHEME model, the same design is applied within each cell of $7 \text{ km} \times 7 \text{ km}$. The saturation threshold of the upper layer – like another tenth of model parameters – is optimized on a set of gauged sub-catchments and the values are afterwards regionalized over the entire Meuse and Scheldt basins using empirical relationships with geographical indices. The soil moisture of the upper layer has been shown to compare well with gravimetric data from a field survey [30].

In figure 5.1 below a grid is shown of the SCHEME hydrological over the Scheldt basin (upstream Antwerp, in blue), and grid cells of H26 intersecting with the Demer catchment (in green).

In this report, the H26 product is compared with the water content of the two soil layers. These results have been obtained for the Demer catchment in the Scheldt basin (Figure 6). The Demer catchment is considered at the gauged station at Molenstede (1775 km²). It is characterized by a fairly flat topography, loamy soils in the upstream part and humid sandy-loamy soils more downstream, and it is mainly covered with crops and pasture.

The spatial resolution of H26 and SCHEME differ both in area and in depth. For this reason, the H26 values have been averaged over grid cells that have an intersection greater than 50% with the catchment. The SCHEME data have been averaged over the vegetation covers and over the catchment. The upper layer of SCHEME has been compared with the first layer of H26. Soil moisture has been expressed in saturation percentage. For SCHEME, the water depth of the conceptual reservoir has been divided by the saturation threshold. For H26, soil moisture index, S , has been further rescaled according to:

$$P_{i,j} = \frac{100(S_{i,j} - \min(S_{i,*}))}{(1 - S_{i,j})} \quad (4)$$

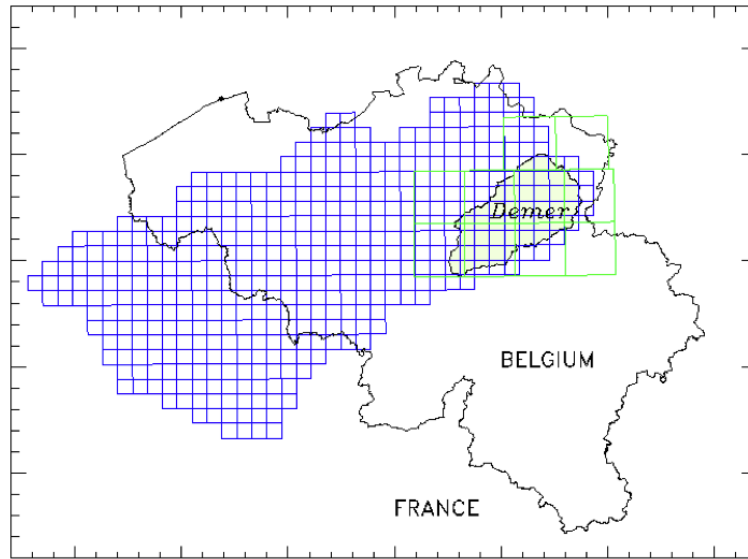


Figure 5.1: Map of Belgium with the watershed of the Demer at Molenstede.

where i refers to the considered layer and j is the day.

The lower layer of SCHEME corresponds to a zone comprising a fraction of the first layer of H26, the second layer and a fraction of the third layer. Therefore, it has been averaged over the three layers using weights defined on the base of the estimated capacity of these three layers and the capacity of the two SCHEME soil reservoirs. Since the capacity of the reservoir corresponding to the saturation zone varies with the month, so do the weights.

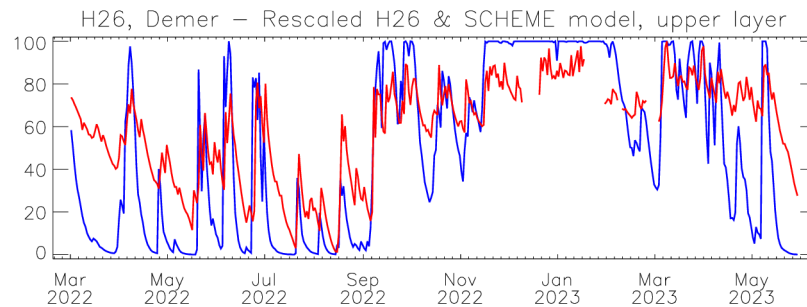
The results are shown in Figures 5.2a and 5.2b as time-series of the percentage of saturation. The upper soil layer of the hydrological model reaches saturation on several occasions (particularly during winter) whereas H26 does not. The capacity of the upper layer of the SCHEME model is about 10 mm over the Demer catchment whereas the capacity of the first layer of H26 is estimated at 18 mm. Most of the events are detected in both series. The time evolution of the saturation of the lower layer of the SCHEME model and the weighted average of the saturation over the H26 soil profile are similar despite the different modelling approaches and the various approximations involved in the comparison. A correlation coefficient of 0.79 is obtained between the first layer of H26 and the upper layer of the SCHEME model. A correlation coefficient of 0.79 is found between the lower layer of the SCHEME model and a weighted average of the values of the three first H26 layers.

5.3. Case study analysis in Bulgaria (NIMH Sofia)

5.3.1. Introduction

The H26 root-zone soil wetness index over Bulgaria was validated over the period 23rd March 2022 to 31st May 2023. The validation was performed by comparing the H26 soil moisture with automatic in situ measurements from 15 stations over the agro-meteorological network of NIMH [31, 32], which are located in Figure 5.3. The climate type of the region is temperate continental and 4 of the stations (above 800 m) are influenced by mountainous climate conditions.

- (a) Saturation percentage of H26 first soil layer (red) and of the SCHEME upper layer (blue) for the Demer



- (b) Saturation percentage of H26 first three layers (weighted average in green) and the SCHEME lower layer (blue)

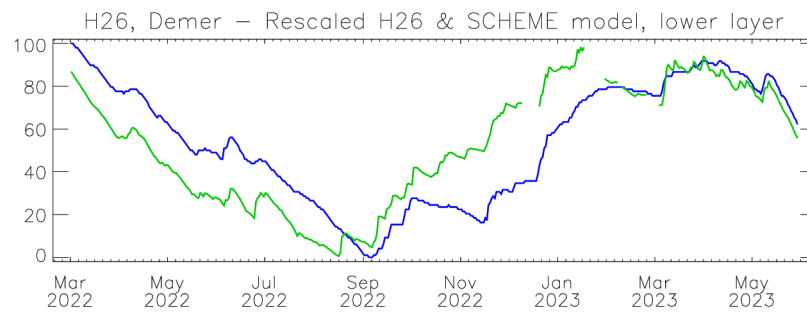


Figure 5.2: Time series of H26 vs SCHEME for (a) upper and (b) lower layers.

5.3.2. Sensor locations

Six stations are equipped with “CS655 Water Content Reflectometer” sensors <https://s.campbellsci.com/documents/es/manuals/cs650.pdf> with 12 cm rods. Two of them, Chirpan and NAO Rozhen, have 2 sensors inserted in the soil at 8 cm depth in the horizontal direction and 2 others in the vertical direction from 40 to 52 cm depth. The remaining 4 stations have one sensor inserted in the vertical direction at 40 to 52 cm depth. All the sensors measure SM values in m³/m³ units. Although sensors can be precisely calibrated to the specific soil properties using laboratory measurements for each site, in this case the factory calibration is used. Sensors measure dielectric permittivity that is converted (by the sensor logic) to volumetric water content using the Topp equation [33]. Four of these stations are located in mountainous areas – NAO Rozhen, res.Sh.Polyana, hut Nadezhda and hut Smirnenski, with the purpose to assess SM evolution in the areas higher than 800 m above sea level. Chirpan station is located in the valley at about 168 m above sea level and Kardzhali station in a hilly area near the town of Kardzhaly. Another 4 stations are equipped with ENVIROSCAN profile sensors, which are measuring at every 10 cm depth: Isparih, Ivaylo, Knezha and Lozen. These sensors are used to validate the H26 profile for layers 2-3 (7-28 cm and 28-100 cm).

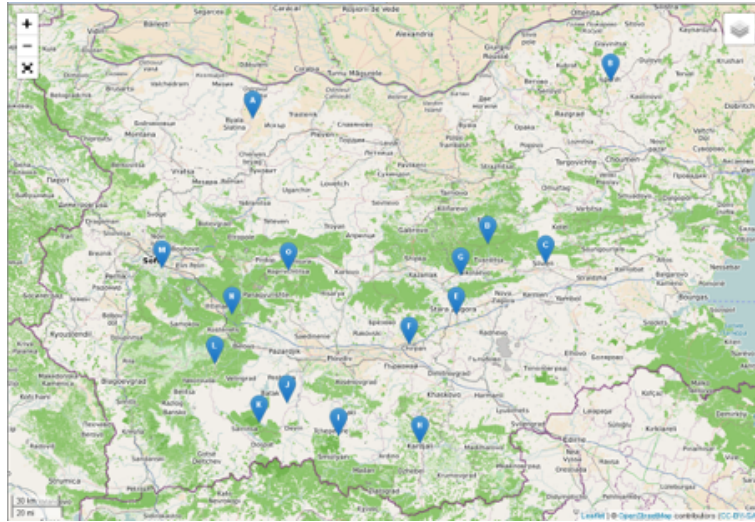


Figure 5.3: Map of Bulgaria with the locations of the automatic sensors.

5.3.3. Data processing

The hourly measured values of CS655, CS650 and ENVIROSCAN sensors data was daily averaged and normalized for the 0-1 m layer:

$$Sensor[0 - 1] = \frac{Sensor - Sensor_{min}}{Sensor_{max} - Sensor_{min}} \quad (5)$$

For the comparison of SM, sensors mounted vertically are compared with integrated H26 values from 2 layers (Layer 2 at 7-28 cm depth and Layer 3 at 28-100 cm depth) to better account for the insertion depth of sensors. Most of the sensors are mounted from 40 to 52 cm depth (in

upper third of H26 layer 3) so the following formula is used:

$$H26^* = (H26_{7-28} + H26_{28-100} * 4) / 5 \quad (6)$$

Because of the highly compacted soil or rocky substrate, three of the sensors (Rozhen, Vetren, Shiroka Polyana) are mounted at a shallow depth of about 25-30 cm. Therefore, a modified formula is used for them:

$$H26^* = (H26_{7-28} * 4 + H26_{28-100}) / 5 \quad (7)$$

Furthermore, H26 values are normalized separately for each location:

$$H26[0 - 1] = \frac{H26^* - H26_{min}^*}{H26_{max}^* - H26_{min}^*} \quad (8)$$

5.3.4. Statistical results

The average statistics for the period 2022/03/23-2023/05/31 are presented in Table 5.1.

Table 5.1: Average statistics for the period 2022/03/23-2023/05/31

Samples	Bias	SD (-)	RMSD (-)	R (-)
6330	-0.034	0.195	0.198	0.790

Statistical analysis of the six CS650-655 sensors shows that most of mountain stations above 1000 m above sea level (Figure 5.3) have slightly lower average yearly statistical scores compared to the stations located below 1000 m above sea level. Furthermore, the seasonal scores in Table 5.3 demonstrate superior average scores during the summer months compared to the winter months. This could be related to frozen conditions during the winter months and at high altitudes. The low scores during the period March-May 2023 could be related to snow melting.

Station name	Chirpan	Rozhen	Sh.Poly.	h.Nadez.	Kardz.	Fotin.	Kopr.	h.Buk.	h.Smirn.	Vetren	Knezha	Isperih	Lozen	Sliven	St.Zag.
Sensor	CS650	CS650	CS655	CS655	CS655	CS655	CS655	CS655	CS655	CS655	ENVIR	ENVIR	ENVIR	CS655	CS655
Ne	42027	45127	47627	64567	44017	47597	71450	41477	47687	42437	3047	23037	64207	41017	42017
at the map	F	I	K	N	H	J	O	D	L	G	A	B	M	C	E
Days samples	426	427	433	389	433	433	369	237	433	217	422	422	433	380	380
A.S.L [m]	168	1759	1500	1024	275	1090	1000	1100	1860	286	136	241	560	256	229
Bias [-]	0.02	-0.04	-0.13	-0.04	0.11	0.02	-0.18	0.02	-0.08	0.03	-0.04	-0.13	-0.02	-0.02	0.02
SD [-]	0.11	0.20	0.18	0.12	0.14	0.31	0.24	0.11	0.21	0.12	0.15	0.23	0.23	0.12	0.15
RMSD [-]	0.11	0.21	0.22	0.13	0.18	0.31	0.30	0.11	0.22	0.12	0.15	0.26	0.22	0.12	0.15
CC	0.95	0.67	0.68	0.93	0.92	0.47	0.65	0.95	0.56	0.90	0.94	0.79	0.81	0.94	0.90

Table 5.2: Results by automatic station equipped with CS650, CS655 or ENVIROSCAN Sensors.

	scores	March. - May 2022	Jun.-Aug. 2022	Sept.-Nov. 2022	Dec. 2022 – Feb.2023	March. - May 2023
15 sensors measure at 30-40 cm depth	Number of days	714	1179	1266	1223	1352
	Bias [-]	-0.053	-0.011	-0.077	-0.076	0.009
	SD [-]	0.206	0.180	0.207	0.222	0.160
	RMSD [-]	0.212	0.180	0.221	0.235	0.160
	CC	0.475	0.740	0.476	0.413	0.117

Table 5.3: Seasonal statistics for the period 2022/03/23-2023/05/31.

6. Conclusion

Firstly, the RZSM-ASCAT-NRT-10km (H26) product has been validated using the temporal correlation of the root zone (0-1 m) against sparse in situ measurements from the International Soil Moisture Network [4]. The in situ measurements from 6 networks belonging to the ISMN were employed, namely SCAN, USCRN and SNOTEL in the USA, SMOSMANIA in southwest France, REMEDHUS in Spain and TERENO in Germany. Averaged over the period, the correlation coefficient (Pearson R) meets the target HSAF performance requirements ($R > 0.65$) for the surface and root-zone SWI for all the networks. As expected, the anomaly correlation coefficients (Ranom) demonstrate generally lower values than the R on average since the autocorrelation from the annual soil moisture cycle is reflected in the R but not in the Ranom. Nevertheless, for the surface and root-zone SWI, the Ranom meets the threshold requirement (> 0.50). The best performances are found in the SMOSMANIA and TERENO network (Ranom exceeding 0.65), which capture well the seasonal cycle of the in situ observations. The most uncertainty (largest confidence intervals) is found over the SNOTEL network in the US, which is affected by frozen conditions over many stations. Overall the validation results for H26 are highly encouraging and demonstrate the benefits of using different validation approaches to assess the performance of a soil moisture data product.

Two case studies were presented. In one case, the soil moisture from H26 was indirectly validated using the SCHEME hydrological model at RMIB, Belgium. The Soil moisture index from H26 was compared with the SCHEME model soil moisture for the Demer catchment (1775 km²) in the Scheldt basin. The upper and lower layers of the scheme model soil moisture were well correlated with H26 ($R > 0.7$). A second case study over Bulgaria (NIMH SOFIA) compared H26 soil moisture with 15 automatic in situ soil moisture stations in the Bulgarian agro-meteorological network. They demonstrated a good level of performance overall, with a Pearson R above 0.65 for the bottom two layers of H26.

7. References

- [1] “Algorithm theoretical baseline document (ATBD), RZSM-ASCAT-NRT-10km (H26),” Tech. Rep. Doc. No: SAF/HSAF/ATBD-26, v0.2, 2021.
- [2] “Product user manual (PUM), RZSM-ASCAT-NRT-10km (H26),” Tech. Rep. Doc. No: SAF/HSAF/PUM-26, v0.1, 2021.
- [3] “Product validation report (PVR), RZSM-ASCAT-NRT-10km (H26),” Tech. Rep. Doc. No: SAF/HSAF/PVR-26, v0.1, 2021.
- [4] W. Dorigo, W. Wagner, R. Hohensinn, S. Hahn, C. Paulik, A. Xaver, A. Gruber, M. Drusch, S. Mecklenburg, P. Oevelen, and A. Robock, “The International Soil Moisture Network: a data hosting facility for global in situ soil moisture measurements,” *Hydrol. Earth Syst. Sci.*, vol. 15, pp. 1675–1698, 2011.
- [5] P. de Rosnay, M. Drusch, D. Vasiljevic, G. Balsamo, C. Albergel, and L. Isaksen, “A simplified Extended Kalman Filter for the global operational soil moisture analysis at ECMWF,” *Quart. J. Roy. Meteor. Soc.*, vol. 139, pp. 1199–1213, 2013.

-
- [6] B. van den Hurk, P. Viterbo, A. Beljaars, and A. Betts, "Offline validation of the ERA-40 surface scheme," in *Technical Memorandum 295*. ECMWF, 2000, [Available online at <http://www.ecmwf.int/publications/>].
 - [7] B. van den Hurk and P. Viterbo, "The Torne-Kalix PILPS 2(e) experiment as a test bed for modifications to the ECMWF land surface scheme," *Global and Planetary Change*, vol. 38, pp. 165–173, 2003.
 - [8] G. Balsamo, A. Beljaars, K. Scipal, P. Viterbo, B. van den Hurk, M. Hirschi, and A. Betts, "A Revised Hydrology for the ECMWF Model: Verification from Field Site to Terrestrial Water Storage and Impact in the Integrated Forecast System," *J. Hydrometeor.*, vol. 10, pp. 623–643, 2009.
 - [9] D. Fairbairn, P. de Ronsay, and P. Browne, "The new stand-alone surface analysis at ECMWF: Implications for land-atmosphere DA coupling," *J. Hydrometeor.*, vol. 20, pp. 2032–2042, 2019.
 - [10] FAO, "'Digital soil map of the world (DSMW)'," in *Technical report*. Food and Agriculture organization of the United Nations, 2003.
 - [11] C. Massari, L. Brocca, L. Ciabatta, T. Moramarco, G. S., C. Albergel, P. De Rosnay, S. Puca, and W. Wagner, "The use of H-SAF soil moisture products for operational hydrology: flood modelling over Italy," *Hydrology*, vol. 2, pp. 2–22, 2015.
 - [12] C. Albergel, C. Rudiger, D. Carrer, J.-C. Calvet, N. Fritz, V. Naeimi, Z. Bartalis, and S. Hasenauer, "An evaluation of ASCAT surface soil moisture products with in situ observations in Southwestern France," *Hydrol. Earth Syst. Sci.*, vol. 13, pp. 115–124, 2009.
 - [13] C. Rudiger, J.-C. Calvet, C. Gruhier, T. Holmes, R. De Jeu, and W. Wagner, "An inter-comparison of ERS-Scat and AMSR-E soil moisture observations with model simulations over France," *J. Hydrometeor.*, vol. 10, p. 431–447, 2009.
 - [14] L. Brocca, S. Hasenauer, T. Lacava, F. Melone, T. Moramarco, W. Wagner, W. Dorigo, P. Matgen, J. Martínez-Fernández, P. Llorens, J. Latron, C. Martin, and M. Bittelli, "Soil moisture estimation through ASCAT and AMSR-E sensors: an intercomparison and validation study across Europe," *Remote Sens. Environ.*, vol. 115, pp. 3390–3408, 2011.
 - [15] G. Schaefer, M. Cosh, and T. Jackson, "The USDA natural resources conservation service soil climate analysis network (SCAN)," *J. Atmos. Oceanic Technol.*, vol. 24(2), pp. 2073–2077, 2007.
 - [16] J. E. Bell, M. A. Palecki, C. Baker, W. Collins, J. Lawrimore, R. Leeper, M. Hall, J. Kochendorfer, T. Meyers, T. Wilson, and H. Diamond, "U.S. Climate Reference Network soil moisture and temperature observations," *J. Hydrometeor.*, vol. 14, pp. 977–988, 2013.
 - [17] J. Calvet, N. Fritz, F. Froissard, D. Suquia, A. Petitpa, and B. Pignat, "In situ soil moisture observations for the CAL/VAL of SMOS: the SMOSMANIA network." in *Geoscience and Remote Sensing Symposium, IGARSS 2007.*, vol. 16 (3). IEEE International, 2007, pp. 1293–1314.

-
- [18] C. Albergel, C. Rudiger, T. Pellarin, J.-C. Calvet, N. Fritz, F. Froissard, D. Suquia, A. Petitpa, B. Piguet, and E. Martin, "From near-surface to root-zone soil moisture using an exponential filter: an assessment of the method based on in situ observations and model simulations," *Hydrol. Earth Syst. Sci.*, vol. 12, pp. 1323–1337, 2008.
- [19] S. Zacharias, H. Bogen, L. Samaniego, M. Mauder, R. Fuß, T. Pütz, M. Frenzel, M. Schwank, C. Baessler, K. Butterbach-Bahl, O. Bens, E. Borg, A. Brauer, P. Dietrich, I. Hajsek, G. Helle, R. Kiese, H. Kunstmann, S. Klotz, J. Munch, H. Papen, E. Priesack, H. P. Schmid, R. Steinbrecher, U. Rosenbaum, G. Teutsch, and H. Vereecken, "A network of terrestrial environmental observatories in germany," *Vadose Zone J.*, vol. 10, pp. 955–973, 2011.
- [20] N. Sanchez, J. Martinez-Fernandez, A. Scaini, and C. Perez-Gutierrez, "Validation of the SMOS L2 soil moisture data in the REMEDHUS network (Spain)," *IEEE Trans. Geosci. Remote Sens.*, vol. 50, pp. 1602–1611, 2012.
- [21] W. Dorigo, A. Xaver, M. Vreugdenhil, A. Gruber, A. Hegyiova, A. Sanchis-Dufau, D. Zamolski, C. Cordes, W. Wagner, and M. Drusch, "Global automated quality control of in situ soil moisture data from the International Soil Moisture Network," *Vadose Zone Journal*, vol. 12, 2013.
- [22] J. Martínez-Fernández and A. Ceballos, "Mean soil moisture estimation using temporal stability analysis," *J. Hydrol.*, vol. 312, pp. 28–38, 2005.
- [23] R. Reichle, G. De Lannoy, Q. Liu, J. Ardizzone, A. Colliander, A. Conaty, W. Crow, T. Jackson, L. Jones, J. Kimball, and R. Koster, "Assessment of the SMAP Level-4 surface and root-zone soil moisture product using in situ measurements," *J. Hydrometeor.*, vol. 18, pp. 2621–2645, 2017.
- [24] C. Albergel, J.-C. Calvet, P. de Rosnay, G. Balsamo, W. Wagner, S. Hasenauer, V. Naemi, E. Martin, E. Bazile, F. Bouyssel, and J.-F. Mahfouf, "Cross-evaluation of modelled and remotely sensed surface soil moisture with in situ data in southwestern France," *Hydrol. Earth Syst. Sci.*, vol. 14, pp. 2177–2191, 2010.
- [25] C. Albergel, W. Dorigo, R. Reichle, G. Balsamo, P. De Rosnay, J. Muñoz Sabater, L. Isaksen, R. De Jeu, and W. Wagner, "Skill and global trend analysis of soil moisture from reanalyses and microwave remote sensing," *J. Hydrometeor.*, vol. 14, pp. 1259–1277, 2013.
- [26] A. Alyaari, W. J.-P., A. Ducharne, Y. Kerr, P. de Rosnay, R. de Jeu, A. Govind, A. Albitar, C. Albergel, M. noz Sabater J., P. Richaume, and A. Mialon, "Global-scale evaluation of two satellite-based passive microwave soil moisture datasets (SMOS and AMSR-E) with respect to Land Data Assimilation System estimates," *Remote Sens. Environ.*, vol. 149, pp. 181–195, 2014.
- [27] C. Draper, R. Reichle, G. De Lannoy, and Q. Liu, "Assimilation of passive and active microwave soil moisture retrievals," *Geophys. Res. Lett.*, vol. 39, 2012.
- [28] F. Bultot and G. Dupriez, "Conceptual hydrological model for an average-sized catchment area, I. Concepts and relationships," *J. Hydrol.*, vol. 29, pp. 251–272, 1976.

-
- [29] —, “Conceptual hydrological model for an average-sized catchment area, II. Estimate of parameters, validity of model, applications.” *J. Hydrol.*, vol. 29, pp. 273–292, 1976.
- [30] E. Roulin, “Statistical correction applied to a water-balance model for the Meuse,” in *E.E. van Loon, and P.A. Troch (eds.), Final Report of the DAUFIN project*. The Netherlands: Wageningen University, 2002, [pp 113-129.].
- [31] V. Georgieva, M. Moteva, and V. Kazandjiev, “CONTEMPORARY IRRIGATION REQUIREMENTS OF MAIZE (GRAIN), GROWN ON CHERNOZEMS IN NORTH BULGARIA.,” in *XXXIV CIOSTACIGR V Conference*. Sofia, Bulgaria: NIMH Sofia, 2011, [Available online at https://www.researchgate.net/publication/324498052_CONTEMPORARY_IRRIGATION_REQUIREMENTS_OF_MAIZE_GRAIN_GROWN_ON_CHERNOZEMS_IN_NORTH_BULGARIA].
- [32] V. Kazandjiev, V. Georgieva, Z. Gagova, and E. Artinian, “Meteorological and Crops State Conditions as Indicator for Validation of Satellite with the Ground Soil Moisture Data,” in *Climate symposium*. Darmstadt, Germany: NIMH Sofia, 2014, [Available online at http://www.theclimatesymposium2014.com/S6_Kazandjiev_Agrometeorological%2B%2B.pdf].
- [33] G. Topp, J. Davis, and A. Annan, “Electromagnetic determination of soil water content: measurements in coaxial transmission lines,” *Water Resources Research*, vol. 16 (3), pp. 574–582, 1980.

Appendices

A. Introduction to H SAF

H SAF is part of the distributed application ground segment of the “European Organization for the Exploitation of Meteorological Satellites (EUMETSAT)”. The application ground segment consists of a Central Application Facilities located at EUMETSAT Headquarters, and a network of eight “Satellite Application Facilities (SAFs)”, located and managed by EUMETSAT Member States and dedicated to development and operational activities to provide satellite-derived data to support specific user communities (see Figure A.1):

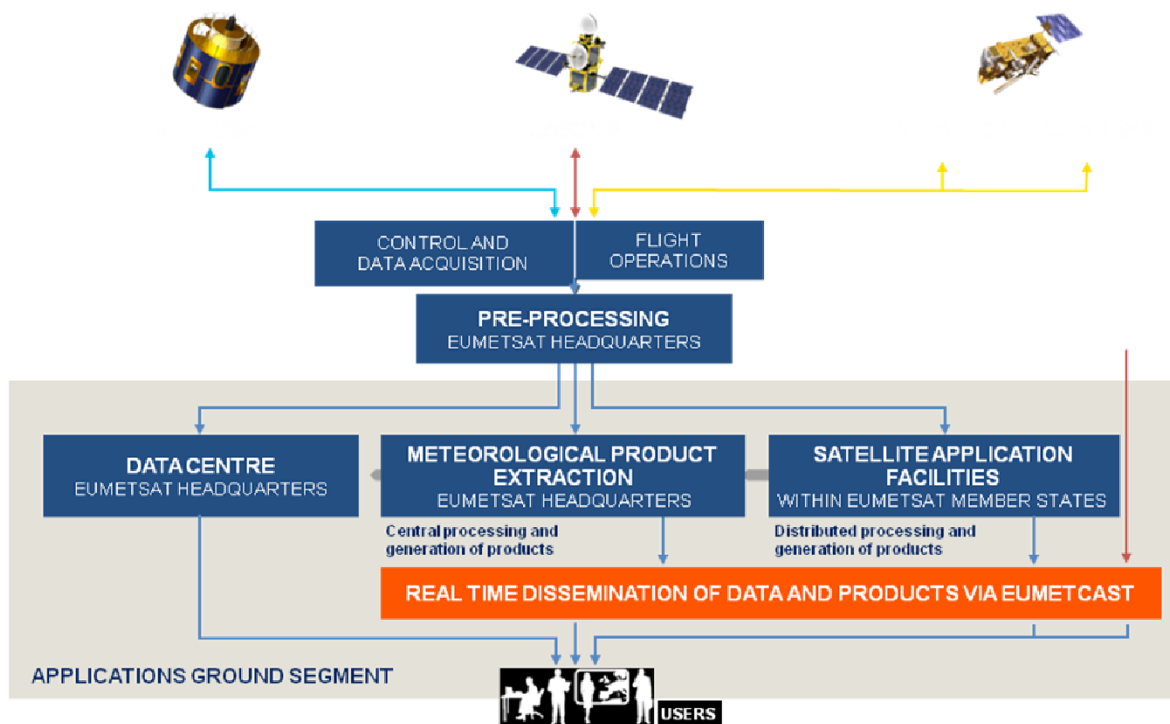


Figure A.1: Conceptual scheme of the EUMETSAT Application Ground Segment.

Figure A.2 here following depicts the composition of the EUMETSAT SAF network, with the indication of each SAF’s specific theme and Leading Entity.

B. Purpose of the H SAF

The main objectives of H SAF are:

- a) to provide new satellite-derived products from existing and future satellites with sufficient time and space resolution to satisfy the needs of operational hydrology, by generating, centralizing, archiving and disseminating the identified products:
 - precipitation (liquid, solid, rate, accumulated);
 - soil moisture (at large-scale, at local-scale, at surface, in the roots region);

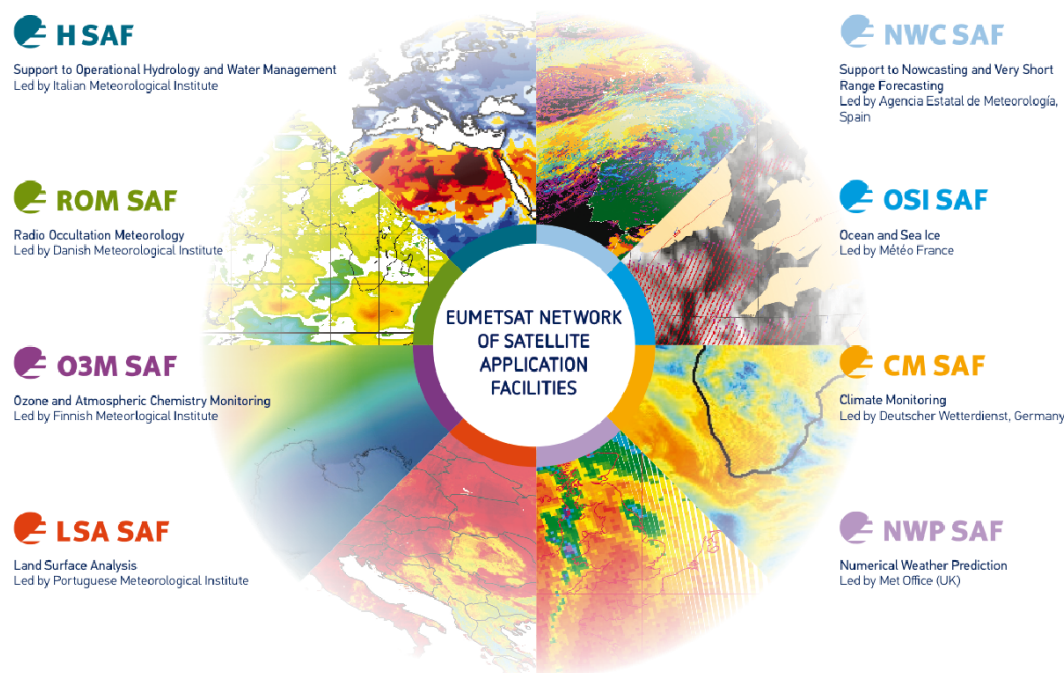


Figure A.2: Current composition of the EUMETSAT SAF Network.

- snow parameters (detection, cover, melting conditions, water equivalent);
- b) to perform independent validation of the usefulness of the products for fighting against floods, landslides, avalanches, and evaluating water resources; the activity includes:
- downscaling/upscaling modelling from observed/predicted fields to basin level;
 - fusion of satellite-derived measurements with data from radar and raingauge networks;
 - assimilation of satellite-derived products in hydrological models;
 - assessment of the impact of the new satellite-derived products on hydrological applications.

C. Products / Deliveries of the H SAF

For the full list of the Operational products delivered by H SAF, and for details on their characteristics, please see H SAF website hsaf.meteoam.it. All products are available via EUMETSAT data delivery service (EUMETCast¹), or via ftp download; they are also published in the H SAF website².

All intellectual property rights of the H SAF products belong to EUMETSAT. The use of these products is granted to every interested user, free of charge. If you wish to use these products, EUMETSAT's copyright credit must be shown by displaying the words "copyright (year) EUMETSAT" on each of the products used.

¹<http://www.eumetsat.int/website/home/Data/DataDelivery/EUMETCast/index.html>

²<http://hsaf.meteoam.it>

D. System Overview

H SAF is lead by the Italian Air Force Meteorological Service (ITAF MET) and carried on by a consortium of 21 members from 11 countries (see website: hsaf.meteoam.it for details)

Following major areas can be distinguished within the H SAF system context:

- Product generation area
- Central Services area (for data archiving, dissemination, catalogue and any other centralized services)
- Validation services area which includes Quality Monitoring/Assessment and Hydrological Impact Validation.

Products generation area is composed of 5 processing centres physically deployed in 5 different countries; these are:

- for precipitation products: ITAF CNMCA (Italy)
- for soil moisture products: ZAMG (Austria), ECMWF (UK)
- for snow products: TSMS (Turkey), FMI (Finland)

Central area provides systems for archiving and dissemination; located at ITAF CNMCA (Italy), it is interfaced with the production area through a front-end, in charge of product collecting. A central archive is aimed to the maintenance of the H SAF products; it is also located at ITAF CNMCA.

Validation services provided by H SAF consists of:

- Hydrovalidation of the products using models (hydrological impact assessment);
- Product validation (Quality Assessment and Monitoring).

Both services are based on country-specific activities such as impact studies (for hydrological study) or product validation and value assessment. Hydrovalidation service is coordinated by IMWM (Poland), whilst Quality Assessment and Monitoring service is coordinated by DPC (Italy): The Services activities are performed by experts from the national meteorological and hydrological Institutes of Austria, Belgium, Bulgaria, Finland, France, Germany, Hungary, Italy, Poland, Slovakia, Turkey, and from ECMWF.